A Resonant Driver for a Piezoelectric Motor

Sam Ben-Yaakov[1*], Evgeny Rozanov[1], Tomer Wasserman[2],
Tzachi Rafaeli[2], Lior Shiv[2] and Gregory Ivensky[1]

[1] Power Electronics Laboratory, Department of Electrical and Computer Engineering Ben-Gurion University of the Negev, P. O. Box 653, Beer-Sheva 84105, ISRAEL. Tel: +972-7-646-1561; Fax: +972-7-647-2949; Email: sby@bguee.ee.bgu.ac.il; Web site: http://www.ee.bgu.ac.il/~pel.

[2] Nanomotion Ltd., P. O. Box 223, Yokneam 20692, ISRAEL. Tel: +972-4-959-0862; Fax: +972-4-959-0995

ABSTRACT

A resonant driver for a Piezoelectric Motor (PZM) is presented, analyzed and tested experimentally. Following a short description of the linear PZM applied in this study, the paper covers the analytical relationships of the buck driven push-pull parallel resonant inverter stage. It is shown that the proposed topology is compatible with the drive requirements of the PZM powered from a low voltage (24V). It is also demonstrated that, unlike simple resonant converters, the proposed topology is relatively insensitive to the resonant component values and that it can tolerate added capacitance as introduced when connecting a PZM to the driver via a long cable.

1. INTRODUCTION

Application of piezoelectric (PZ) motors [1, 2] is limited, among other things, by the lack of inexpensive drivers that will match the performance and low cost of the PZ motors. In this paper we describe a newly developed PZ motor resonant driver that has many advantages over the present solutions. First we describe the linear PZM for which the driver was developed, present its simplified electrical equivalent circuit and give the drive requirement. The classical approach of a series resonant inverter is then covered, pointing to its limitations. We present the proposed Push-Pull Resonant Inverter (PPRI) and derive its basic mathematical operational relationships. Finally, we show simulation and experimental results and discuss the merits and drawback of the PPRI as compared to the classical series resonant inverter approach.

2. THE LINEAR PIEZOELECTRIC MOTOR

The basic operation of the Nanomotion Ltd. PZM hinges on the flexure and linear expansion of a PZ slab (Fig. 1). The PZ element has three electrodes, two (A & B) are deposited on one surface (Fig. 1) while the third one (C) is deposited on the bottom surface of the PZ element. Electrodes 'A' and 'B' are of two parts. Each part is placed diagonally on the upper PZ surface (Fig. 1). When an electrical excitation is imposed between 'A' or 'B' electrodes and 'C' electrode, the element will flex and expand and consequently the stem attached to one end of the PZ element, will move in the 'X' and 'Y' dimensions (Fig. 1). Hence when the PZ element of Fig. 1 is placed against a flat surface, as shown in Fig. 2, it will exert mechanical force on the surface and can move the platform if the PZ is mechanically anchored. Excitation the A-C electrodes will cause movement to one direction while excitation of the B-C electrodes will cause movement in the other direction. For rotary motion the PZM is placed against the circumference of a wheel.

From an electrical point of view, the PZM can be represented to a first approximation by an RC network (Fig. 3). This approximation is valid around the operating frequency. The required motor excitation for full power of PZ element

* Corresponding author

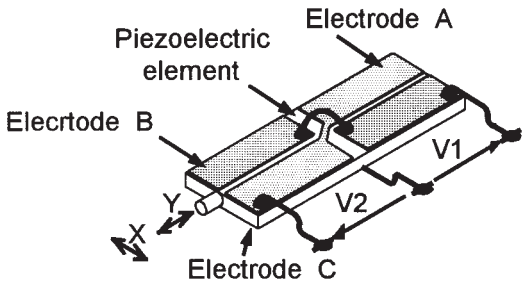

Fig. 1. Electrode configuration in a piezoelectric element of a PZM operating in longitudinal plus flexural modes. (Nanomotion Ltd., Israel)

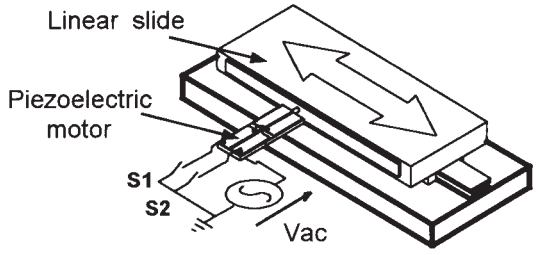

Fig. 2. Method used to generate a linear motion by the piezoelectric element shown in Fig. 1.

is 250Vrms at about 40kHz. Being resonant element [1, 2] only the relevant resonant frequencies will develop force. Hence, the ideal drive for the PZM is a sinusoidal waveform since the non relevant harmonics are ineffective and only increase the circulating reactive current. Nonetheless some distortion (30-50%) can be tolerated without ill effect.

3. THE CONVENTIONAL APPROACH

Conventional drivers for a PZM [3] are normally based on a resonant network. In such a configuration the PZM is connected parallel to the capacitor of a series LC-circuit which is fed from the ac network (Fig. 4) or a squarewave drive. To achieve a sinusoidal waveform and to obtain a voltage gain, the LC-circuit is normally operated near resonance. The peak of the first harmonic of the motor voltage $V_{m(1)pk}$ is governed by the equation:

$$V_{m(1)pk} = \frac{V_{s(1)pk}}{\sqrt{[1-(\frac{f_s}{f_{ro}})^2]^2 + (\frac{f_s}{f_{ro}})^2 \frac{1}{Q^2}}} \qquad (1)$$

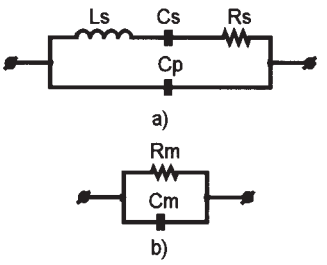

Fig. 3. Equivalent circuit of a piezoelectic element. (a) general circuit for one vibration mode. (b) simplifies equivalent circuit at PZM operating frequency.

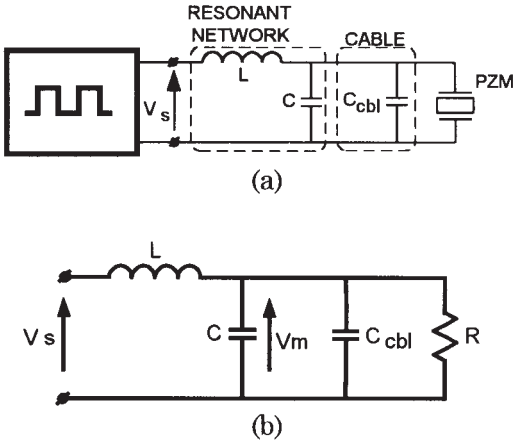

Fig. 4. LC type PZM driver. (a) system configuration. (b) equivalent circuit.

where $V_{s(1)pk}$ is the peak of the first harmonic of the supply voltage, f_s is the driver frequency, f_{ro} is the resonant frequency of ideal LC_Σ circuit:

$$f_{ro} = \frac{1}{2\pi\sqrt{LC_\Sigma}} \qquad (2)$$

C_Σ is the sum of capacitances of the driver (C), of the cable (C_{cbl}) and of PZM (C_m):

$$C_\Sigma = C + C_{cbl} + C_m \qquad (3)$$

and Q is the quality factor:

$$Q = \frac{R_m}{\sqrt{\frac{L}{C_\Sigma}}} \qquad (4)$$

In practical cases cable is of variable length and therefore its capacitance C_{cbl} may have different values. As a result, C_Σ (eq. (3)) is not constant, a fact that might deteriorate the performance of the

circuit due to the movement of the resonant frequency.

Eq. (1) was used to examine the relative variation of the peak of the first harmonic of the motor voltage ($\Delta V_{m(1)pk} / V_{m(1)pk}$) as a function of the relative capacitance variation ($\Delta C_\Sigma / C_\Sigma$):

$$\frac{\Delta V_{m(1)pk}}{V_{m(1)pk}} = \sqrt{\frac{[1-(\frac{f_s}{f_{ro}})^2]^2 + (\frac{f_s}{f_{ro}})^2 \frac{1}{Q^2}}{[1-(\frac{f_s}{f_{ro}})^2(1+\frac{\Delta C_\Sigma}{C_\Sigma})]^2 + (\frac{f_s}{f_{ro}})^2 \frac{1}{Q^2}}} - 1 \qquad (5)$$

where $\Delta V_{m(1)pk}$ and ΔC_Σ are increments of $\Delta V_{m(1)pk}$ and C_Σ respectively. The resonant frequency f_{ro} and the quality factor Q in (5) correspond to the value C_Σ before the change.

Applying (5), the dependence of $\frac{\Delta V_{m(1)pk}}{V_{m(1)pk}}$ on $\frac{f_s}{f_{ro}}$ for different values of Q for $\frac{\Delta C_\Sigma}{C_\Sigma} = 0.1$ was calculated (Fig. 5) . It is clear that the relative change $\frac{\Delta V_{m(1)pk}}{V_{m(1)pk}}$ can be much higher than $\frac{\Delta C_\Sigma}{C_\Sigma}$, especially at high values of the quality factor Q. However, high Q is needed for good filtering of the squarewave normally used as drive and to achieve the voltage gain needed in practical circuit. It is thus clear that the high sensitivity of the output voltage to capacitance changes makes the conventional LC driver useful only when the total capacitances is constant. However in many practical cases capacitance changes are expected due to many factors: variable cable length, temperature rise of the PZ element which increases its capacitance, practical spread of components' value etc. In these situations, the conventional LC driver is clearly disadvantageous.

4. THE PUSH PULL PARALLEL RESONANT INVERTER (PPRI)

The proposed resonant driver is built around a current fed PPRI [4], [5] and a front end Buck converter (Fig. 6). The function of the Buck converter is to control the average voltage fed to the PPRI and hence the voltage across the motor. The PPRI is run at a constant frequency and the MOSFET switches Q1 and Q2 are driven at 50% duty cycle. The resonant circuit comprises an

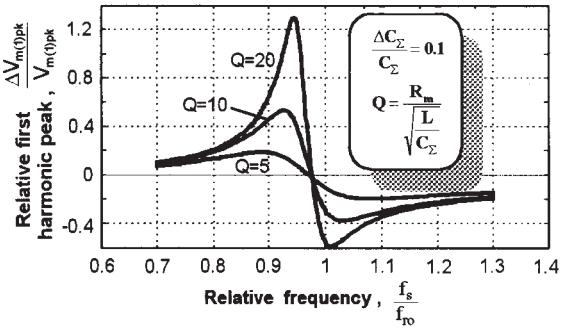

Fig. 5. Output voltage sensitivity of the LC driver to changes in total capacitance as a function of operating frequency. Y axis = relative change in voltage amplitude due to a relative change of 0.1 in total circuit capacitance.

inductor L, a capacitor C, capacitance of the cable C_{cbl}, capacitance C_m and resistance R_m of the motor (Fig. 6). In practice, the magnetization inductance of the transformer T serves as the resonant inductor L.

The operation of the PPRI can be described by the simplified circuit diagrams of Fig. 7. The input inductor L_{in} (Fig. 6) is replaced here by a current source I_{in} under the assumption:

$$L_{in} >> \frac{L}{n^2} \qquad (6)$$

where n is the transformer turns ratio. C', C_{cbl}', C_m', L' and R_m' are capacitances, inductance and resistance reflected to the primary of the transformer:

$$C' = \frac{n^2 C}{4} \quad (7), \quad C_{cbl}' = \frac{n^2 C_{cbl}}{4} \qquad (8)$$

$$C_m' = \frac{n^2 C_m}{4} \quad (9), \quad L' = \frac{4L}{n^2} \quad (10), \quad R_m' = \frac{4R_m}{n^2} \quad (11)$$

The drive period T_s must be longer than the resonant period T_r of the real $LC_\Sigma R_m$ circuit (as before C_Σ is the sum of capacitances (eq. (3)):

$$T_s > T_r = \frac{2\pi\sqrt{LC_\Sigma}}{\sqrt{1-\frac{1}{4Q^2}}} \qquad (12)$$

where Q is the quality factor (eq. (4)).

Each half cycle of the PPRI comprises two operational modes: a resonant mode when one transistor is conducting and both antiparallel diodes are not conducting (Fig. 7b) and a boost mode when the resonant tank is shorted through the conducting transistor and the diode connected antiparallel to

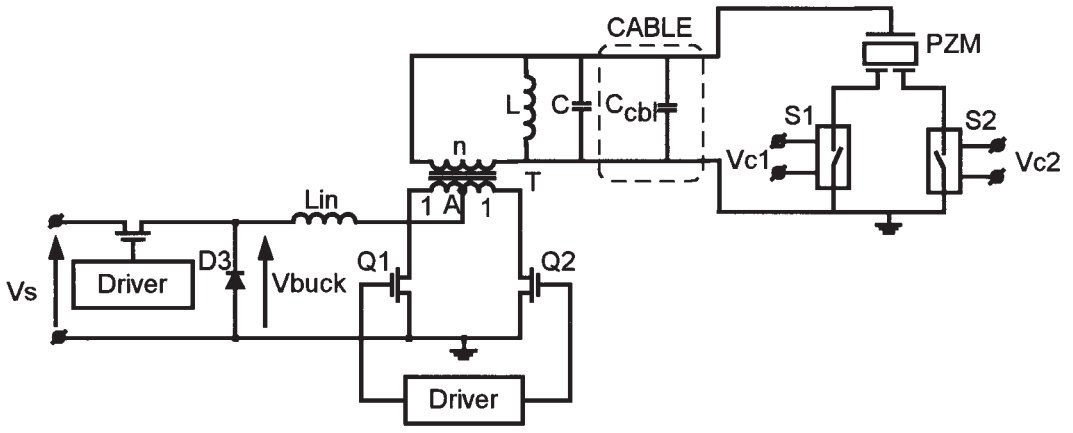

Fig. 6. Basic configuration of proposed PPRI driver. S_1 , S_2 control direction of motion (see Figs. 1 & 2)

the other transistor (Fig. 7c). The duration of the boost mode is dependent on the difference between the drive period T_S and the resonant period T_r. As a result of these two modes, the voltage across the motor v_m will be nearly a sinewave with some dead time between the two half cycles (Fig. 8). The dead time can be reduced by matching the resonant frequency $f_r = 1/T_r$ to the drive frequency $f_s = 1/T_s$.

We assume that switches, diodes, transformer, inductor and capacitors are ideal and that the waveform of capacitor's voltage (i. e. the voltage across the motor v_m) during the resonant mode is a sinusoidal:

$$v_m = V_{mpk} \cos(\frac{\pi}{\lambda}\vartheta) \qquad (13)$$

where V_{mpk} is the peak motor voltage, $\vartheta = 2\pi f_r t$ is normalized time in radians with zero value when $v_m = V_{mpk}$, t is the time and λ is normalized duration of the resonant mode:

$$\lambda = \pi \frac{T_r}{T_s} = \pi \frac{f_s}{f_r} \qquad (14)$$

The peak motor voltage V_{mpk} is found from the condition that the average voltage across the ideal input inductor L_{in} is zero. Therefore the average voltage at point 'A' (Figs. 6,7) V_{Aav} is equal to the average voltage across the diode D_3 of the buck converter V_{buck} :

$$V_{Aav} = V_{buck} = D_{buck} V_s \qquad (15)$$

where D_{buck} is the duty cycle of the buck converter and V_S is the supply voltage of the driver (Fig. 6).

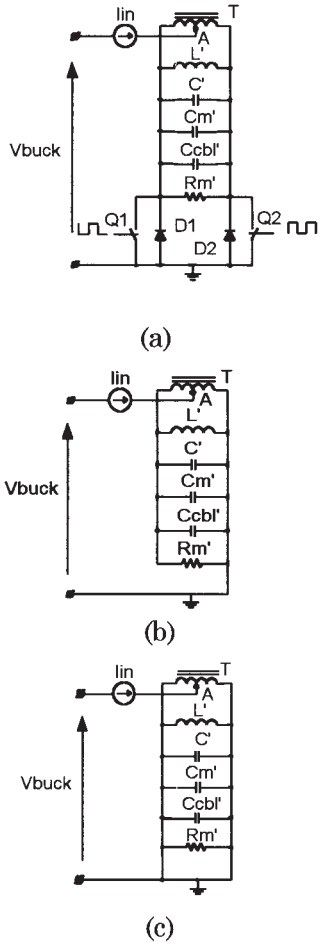

Fig. 7. Equivalent circuit of the PPRI driver (Fig. 6) with the secondary reflected to primary.
(a) general circuit. (b) resonant mode.
(c) boost mode.

On the other hand, V_{Aav} can be obtained from (13):

$$V_{Aav} = \frac{1}{\pi}\int_{-\lambda/2}^{\lambda/2} \frac{V_{mpk}}{n}\cos(\frac{\pi}{\lambda}\vartheta)d\vartheta = \frac{2\lambda}{\pi^2}\frac{V_{mpk}}{n} \quad (16)$$

From (14)-(16) we find:

$$V_{mpk} = nV_{buck}\frac{\pi}{2}\frac{f_r}{f_s} = nD_{buck}V_s\frac{\pi}{2}\frac{f_r}{f_s} \quad (17)$$

Applying (13) the peak of the first harmonic of the motor voltage can was derived:

$$V_{m(1)pk} = \frac{2}{\pi}\int_{-\lambda/2}^{\lambda}(V_{mpk}\cos(\frac{\pi}{\lambda}\vartheta)\cos\vartheta)d\vartheta =$$

$$= V_{mpk}\frac{4}{\pi}\frac{1}{\pi/\lambda - \lambda/\pi}\cos(\lambda/2) \quad (18)$$

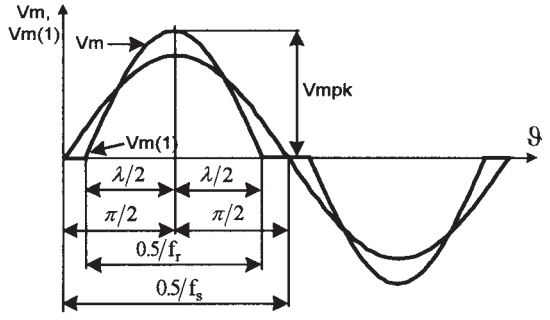

Fig. 8. Output voltage waveform (PZM voltage) of the PPRI driver.

Taking into account (14) and (17) we transform (18) into:

$$V_{m(1)pk} = \frac{2\cos(\lambda/2)}{1-(\lambda/\pi)^2} = \frac{2\cos(\frac{\pi}{2}\frac{f_s}{f_r})}{1-(f_s/f_r)^2} \quad (19)$$

Eqs.(19) and (12) are used to derive the dependence of $\frac{\Delta V_{m(1)pk}}{V_{m(1)pk}}$ on $\frac{\Delta C_\Sigma}{C_\Sigma}$ (Fig. 5) :

$$\frac{\Delta V_{m(1)pk}}{V_{m(1)pk}} = \frac{[1-(\frac{f_s}{f_r})^2]\cos[\frac{\pi}{2}\frac{f_s}{f_r}\sqrt{1+\frac{\Delta C_\Sigma}{C_\Sigma}}]}{[1-(\frac{f_s}{f_r})^2(1+\frac{\Delta C_\Sigma}{C_\Sigma})]\cos(\frac{\pi}{2}\frac{f_s}{f_r})} - 1 \quad (20)$$

This relationship is shown in Fig. 9 as a function of $\frac{f_s}{f_r}$ for $\frac{\Delta C_\Sigma}{C_\Sigma} = 0.1$. It is seen that in this case $\frac{\Delta V_{m(1)pk}}{V_{m(1)pk}}$ is very small, much lower than $\frac{\Delta C_\Sigma}{C_\Sigma}$. Hence the proposed PPRI topology is clearly advantageous in situations that the capacitance is not constant. That is a very important advantage of the proposed driver.

5. RESULTS AND DISCUSSION

A resonant driver was designed for an SP1 PZM (Nanomotion Ltd.). The parameters of the PZM were as follows: drive frequency 39.6kHz, maximum drive voltage: 260Vrms, equivalent circuit of PZM: C_m=1.3nF, R_m=3.75kΩ. Nominal supply voltage to driver 24V.
The simulation and experimental results of the PPRI driver were found to be in excellent agreement. Typical waveforms of the motor voltage are shown in Fig. 10.

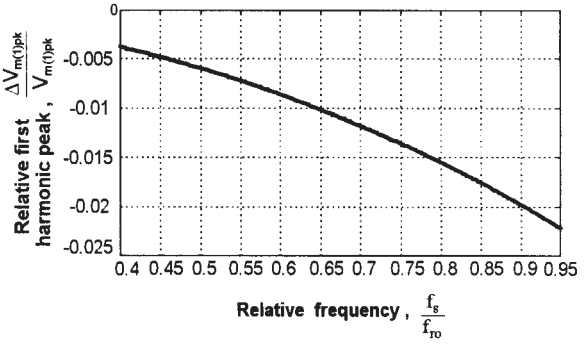

Fig. 9. Output voltage sensitivity of PPRI driver to changes in total capacitance as a function of operating frequency. Y axis = relative change in voltage amplitude of the first harmonics due to a relative change of 0.1 in total circuit capacitance.

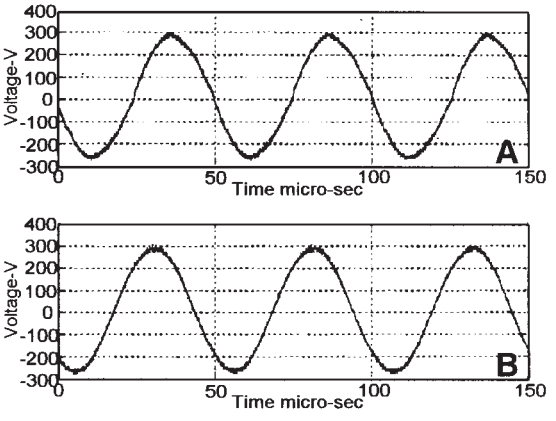

Fig. 10. PZM voltage when driven by proposed PPRI drive. (A) 3 m cable (0.6 nF). (B) 10 m cable (2 nF).

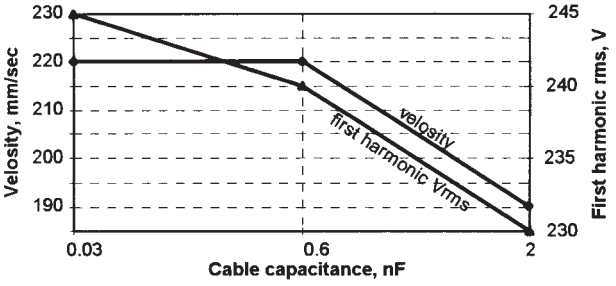

Fig. 11. PZM velocity and rms of first harmonics when driven by proposed PPRI driver, as a function of added capacitance.

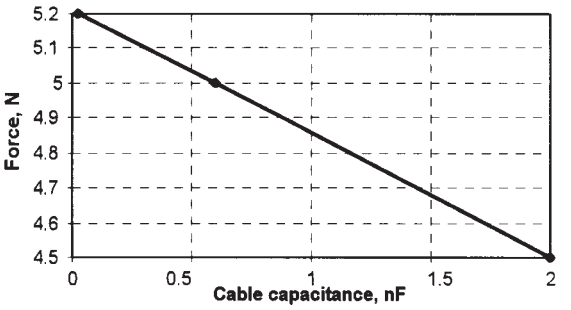

Fig. 12. PZM force when driven by proposed PPRI driver, as a function of added capacitance.

The robustness of the topology against capacitance changes was tested by adding a capacitance across the PZM. The effect of this extra capacitance on the motors' voltage, motor velocity
(Fig. 11) and motor force (Fig. 12) were found to be rather small even when a large capacitance is added (2nF, corresponding to a cable length of 10m).
The results of this study suggest that the proposed PPRI topology is much less sensitive to capacitance variations than the conventional LC driver. Other advantages are also important:

1. In both the conventional LC driver and the proposed PPRI, the relative capacitance change $(\Delta C_\Sigma / C_\Sigma)$ can be made small by purposely increasing C_Σ. This however will reduce the characteristic impedance and hence increase the reactive current. The advantage of the PPRI in this case will be in the fact that the circulating current passes through the switches only during the boost period [5]. In the LC driver all the circulating current passes through the switches. Consequently, everything being equal, the PPRI is expected to have a higher efficiency.
2. The incorporation of a transformer in the basic design of the PPRI enables one to use any input voltage to generate the rather high (and floating) voltage needed to drive the PZM.
3. From the electronics point of view, the fact that the drive of the push pull transistors is referred to the 'ground' of the circuit simplifies the design. The circuitry involved is rather simple and can be realized by low cost commercial components.
4. Motor voltage regulation can be easily achieved by just adding an extra switch to form the Buck front end. Motor voltage is linear with the duty cycle, making the control circuitry simple.

6. CONCLUSIONS

The proposed resonant driver is shown to be a viable choise for PZM applications. The main advantages of the proposed PPRI topology is relative insensitivity to added capacitance, simplicity and ease of control. The mathematical expression developed in this study can be easily used as design guides for this topology.

REFERENCES

[1] W. R. Chynoweth, J. F. Elliott, H. W. Katz, E. B. Mullen, C. A. Rosen, N. Schwartz, B. Silverman, C. F. Spitzer, S. W. Tehon, H. J. Venema, *"Solid state magnetic and dielectric devices"*, New York, John Wiley & Sons, Inc., 1959.

[2] H. P. Shoner, "Piezoelectric motors and their application," *European Trans. on Electrica Power Engineering*, vol. 2, n. 6, November/ December, 1992, pp. 367-371.

[3] Faa-Jeng Lin, "Fuzzy adaptive model - following position control for ultrasonic motor", *IEEE Trans. on Power Electronics*, vol. 12, n. 2, March 1997.

[4] G. Ivensky, A. Abramovitz, M. Gulko, S. Ben-Yaakov, "A resonant dc-dc transformer", *IEEE Trans. on Aerospace and Electronic Systems*, vol. 29, n. 3, July 1993, pp. 926-934.

[5] M. Gulko, S. Ben-Yaakov, "Current-sourcing push-pull parallel-resonance inverter (CS-PPRI): theory and application as a discharge lamp driver", *IEEE Trans. on Industrial Electronics,* vol. 41, n. 3, June 1994, pp. 285-291.